

Merging In-Solution X-ray and Neutron Scattering Data Allows Fine Structural Analysis of Membrane-Protein Detergent Complexes

Gaëtan Dias Mirandela, Giulia Tamburrino, Miloš T. Ivanović, Felix M. Strnad, Olwyn Byron, Tim Rasmussen, Paul A. Hoskisson, Jochen S. Hub, Ulrich Zachariae, Frank Gabel, and Arnaud Javelle

Supplementary Information

Experimental procedures

Protein purification and stability: AmtB(His₆), cloned into the pET22b vector¹, was overproduced and purified as described previously¹ except 0.03% (0.58 mM) of n-Dodecyl- β -D-Maltoside (DDM) was used instead of 6 mM *N,N*-dimethyldodecylamine-*N*-oxide (LDAO) in the final Size Exclusion Chromatography (SEC) buffer (Tris/HCl 50mM, pH 7.8, NaCl 100 mM, 0.58 mM DDM). AmtB was kept in SEC buffer at 4°C for subsequent characterisation. AmtB stability was assessed before and after each SAS experiment by SEC using a Superdex 200 10/300 (Ge Healthcare) gel filtration column (Figure S6).

Size Exclusion Chromatography/Multiple Angle Light Scattering (SEC-MALS) analysis: SEC-MALS analysis of the AmtB-DDM complex was carried out using Superdex 200 10/300 column (Ge Healthcare) attached on an Agilent 1100 HPLC system. 70 μ l of AmtB at 75 μ M in SEC buffer was injected at a flow rate of 0.5 ml/min. Light scattering, refraction index and absorbance at 280 nm were measured using a multi-angle light scattering mini DAWN TREOS detector (Wyatt Technology), a refractometer Optilab T-rEX detector (Wyatt Technology) and a Jasco UV-2077 Plus UV/vis spectrophotometer respectively. We used the ASTRA software package version 5.3.2.10 (Wyatt Technologies) to import the signals from the three detectors and analysed the data according to Slotboom *et al.* (2008)².

Analytical Ultra Centrifugation (AUC): AmtB at 10, 22 and 87 μ M was submitted to sedimentation velocity using a Beckman Coulter Optima XL-I analytical ultracentrifuge mounted with an An-50 Ti 4-hole rotor (49000 rpm at 4°C). The reference buffer used was the SEC buffer without detergents (50 mM Tris pH 7.8, 100 mM NaCl). Data were acquired every 6 min for 12 hrs, with interference and absorbance optics and were subsequently analysed using SEDFIT³ with the continuous *c*(*s*) distribution model. SEDNTERP was used

to determine the molar mass (46 647 g/mol) and the partial specific volume (0.749 ml/g) of AmtB. The partial specific volume of DDM used was 0.82 ml/g. The viscosity (1.567 cP) and the density (1.00557 g/ml) of the SEC buffer were determined using SEDNTERP. The ratio of detergent bound to the protein and the molecular weight of the complex (Table S1) were calculated using a method described previously.⁴

Micro-Scale Thermophoresis (MST): AmtB(His₆) was labelled using the kit Monolith His-Tag according to manufacturer instructions (NanoTemper Technologies). Labelled samples of AmtB in the concentration range [6 μ M-200mM] were loaded into 16 hydrophobic coating grade capillaries and analyzed using the Monolith NT.115 (NanoTemper Technologies) analyser. The data were processed using the MO.Affinity Analysis software v2.2.4 (NanoTemper Technologies) as previously described.⁵

Characterisation of the sample: SAS experiments are very demanding in terms of sample quality⁶⁻⁷, therefore, before recording SAS data, we assessed the purity and monodispersity of the samples as follows: the mass of the complex calculated from our SEC-MALS analysis are constant across the elution peak (Figure S1). Secondly, SDS page and SEC analyses of our sample before and after the SAS experiments show that the protein is pure and stable for weeks at 4°C (Figure S6). Finally, to ensure that the protein was purified in an active form, we measured AmtB NH₄⁺ binding activity by microscale thermophoresis. Clear NH₄⁺ dependent binding activity (K_d 0.6 mM) was measured, which indicates that AmtB is correctly folded and active (Figure S3). Taken together, these results show that our sample is pure, monodisperse and that the protein is active in detergent. Hence our sample is highly suitable for SAS analysis.

Molecular Dynamics simulations:

System preparation: The AmtB crystal structure at 1.35 Å obtained by Kademi *et al.* (PDB ID: 1U7G)⁸ was used for the molecular dynamics simulations. The protein was processed using the CHARMM-GUI web interface.⁹⁻¹⁰ The mutations F68S, S126P, and K255L inserted in the crystallographic construct were reverted to the wild-type, all the selenomethionine modifications were changed back to methionine, and the N- and C-terminal residues were capped using acetyl and N-methyl amide groups, respectively. The protein was initially embedded in a DDM bilayer using CHARMM-GUI Membrane Builder plugin.¹¹⁻¹² The system was subsequently solvated in water and K⁺ and Cl⁻ ions were used to neutralise the system and reach a salt concentration of 50 mM. In-house code was then used to remove excess DDM molecules and to form a detergent torus around the protein of 260, 280, 300, 320, 340 and 360 DDM molecules, respectively, in order to reflect the experimental conditions.

Molecular dynamics simulations: All molecular dynamics simulations were performed with the GROMACS 5.1.4 software package.¹³⁻¹⁴ The CHARMM36 force field was used for the protein, the ions, and DDM.¹⁵⁻¹⁶ The water molecules were modelled with the TIP3P model.¹⁷ Water bonds and distances were constrained by the Settle method¹⁸, and all other bonds by the LINCS method.¹⁹ After a steepest descent minimization, the system was equilibrated by six consecutive equilibration steps with position restraints on heavy atoms of 1,000 kJ/mol*nm². The first three equilibration steps were carried under a NVT ensemble using a Berendsen thermostat to keep the temperature at 310 K. The subsequent steps were conducted under a NPT ensemble, switching on a Berendsen barostat²⁰ with isotropic coupling, to keep the pressure at 1 bar. Production molecular dynamics simulations

were carried using a v-rescale thermostat²¹ with a time constant of 0.2 ps, and a Berendsen barostat with isotropic coupling. A Verlet pair-list scheme was used for describing non-bonded interactions, and two different cut-off values, of 1.2 Å and 1.5 Å were tested; no significant difference was observed between these two. A timestep of 2 fs was used throughout the simulations. The first 70 ns of production simulations were discarded from the analysis to allow rearrangement of the DDM molecules around the protein.

SEC-SAXS analysis: Synchrotron SAXS data were collected on the B21 bioSAXS beamline at the DIAMOND Synchrotron. The exact same conditions were used than for the SEC-MALS analysis in terms of sample, column and running conditions. 50 µl of AmtB at 75 µM were injected into the SEC-system. The running buffer used was 50 mM Tris pH 7.8, 100 mM NaCl and 0.03% DDM. 15 frames of the elution peak corresponding to the membrane protein were averaged and subtracted to the running buffer using ScÅtter software. 57 frames corresponding to the buffer curve were averaged prior to the subtraction. SAXS data were collected in 255 time frames with 3 s per frame (13 min in total). The scattering images were averaged and the buffer scattering intensities subtracted using the program ScÅtter and the same program was used to evaluate the radius of gyration (R_g). The data-collection parameters are presented in Table S2.

SAXS curve predictions. SAXS curves were computed using the explicit-solvent calculations described previously²², as implemented in the WAXSiS method.²³ Accordingly, a spatial envelope was constructed around the AmtB-DDM complex, such that the distance of the envelope's vertices have a distance of 6 Å from all atoms in all simulation frames. Because the detergent exhibited substantial fluctuations, this procedure yielded an envelope that had a larger distance from the complex in most of the MD frames, suggesting that solvent density modulations due to the hydration layer were captured by the envelope volume. The spherical average was conducted using 1,200 Q-vectors per absolute value of the scattering vector Q . $Q = (4\pi \sin(\theta)/\lambda)$, where 2θ is the scattering angle. The bulk solvent density was corrected to 334 e/nm³ to correct for the slightly incorrect density of the CHARMM-modified Tip3p model, as described previously.²²

Explicit-solvent SANS predictions. We extended the WAXSiS method, which was originally developed for small- and wide-angle X-ray scattering calculations, to allow the calculation of SANS curves. The calculations were identical to the original WAXSiS method²² except that atomic form factors were replaced by the coherent neutron scattering lengths. The neutron scattering length density was corrected as previously described²², such that the electron density of the solvent was 334 e/nm³. At non-zero relative D₂O concentration c_{D_2O} , the neutron scattering lengths of polar hydrogen atoms of protein, detergent, and water were taken as $b = c_{D_2O}b_D + (1-c_{D_2O})b_H$, where b_D and b_H denote the coherent scattering lengths of deuterium and hydrogen, respectively. Here, we defined hydrogen atoms as polar if they are bound to one of the elements O, N, S, or P. Hydrogen atoms of the backbone amine groups were assumed to be deuterated with 10% reduced probability, $b' = 0.9c_{D_2O}b_D + (1-0.9c_{D_2O})b_H$, as done previously.²⁴⁻²⁵ As a control, we tested the effect of randomly assigning b_D and b_H to polar hydrogen atoms according to the given D₂O concentration, with new random assignments in every MD frame. This protocol models the solution ensemble with heterogeneous random deuteration, as present under experimental conditions. As can easily be shown from the Debye equation, this protocol leads to a constant offset in the intensity curve (independent of Q). Since (i) we adjust the constant offset to account for the incoherent

scattering background, and (ii) random deuteration assignments lead to slower convergence of the SANS intensities, we used the simplified definition with constant, not randomly-assigned, neutron scattering lengths for this work.

Small Angle Neutron Scattering data measurement and analysis: To ascertain the reproducibility and the quality of our measurements, two independent set of SANS data were measured (September 2016 and March 2018) using two batches of AmtB purified independently. SANS experiments were conducted at 6°C using the large dynamic range diffractometer D22 at the Institut Laue-Langevin (Grenoble, France) in Hellma® quartz cuvettes 100QS with 1 mm optical pathlength. 300 µl of samples at a concentration of 110 µM were extensively dialysed (3 times 12 hrs) against the size-exclusion chromatography buffer (50 mM Tris pH 7.8, 100 mM NaCl, 0.03% DDM and D₂O as required) and used for the SANS experiment. The final dialysis buffer was used in the SANS experiment as the reference and subtracted to the protein signal. The samples were recorded at a 4 m/4 m detector/collimator distance, using a neutron wavelength of $\lambda=6 \text{ \AA}$. For each condition, H₂O/D₂O buffers, the empty beam, an empty quartz cuvette as well as a boron sample (electronic background) were measured. Exposure times varied between 20 min (empty cell, boron) and 3 hrs for the protein samples and buffers. Transmissions were measured for 1 min. The raw data were reduced (detector efficiency, electronic background and angular averaging) using a standard ILL software package. Finally, the corrected scattered intensities $I(Q)$ ($Q=(4\pi/\lambda) \sin \theta$, where 2θ is the scattering angle, from the different Q -ranges and the respective buffer signals were subtracted using the program PRIMUS from the ATSAS suite.²⁶ The data-collection parameters are presented in Table S2.

Contrast Variation Series: The contrast match point of DDM was experimentally determined by measuring SANS contrast series of DDM (5 mg/ml) at 0, 20, 40, 60, 80 and 100 % D₂O and used to plot $(I(0)/(T_s C))^{1/2}$ as a function of percentage of D₂O in the solvent (T_s is the measured sample transmission). The DDM contrast match point (22.2%) was determined by the intersection of a linear fit through all points with the abscissa as previously described.²⁷

Guinier plot: Guinier plots were used to calculate the R_g based on the following equation: $\ln[I(Q)] = \ln I(0) - 1/3(R_g^2 * Q^2)$, with $QR_g < 1.3$. AmtB molecular weight, was determined from the $I(0)$ intensity at 22% D₂O using absolute calibration against H₂O under the assumption that the detergent (free micelles and bound) had a negligible contribution at the contrast match point according to Compton *et al.*, (2011)²⁷(Figure S5 and Table S1).

MONSA multiphase modelling: The multiphase volumetric analysis using MONSA²⁸⁻²⁹ (extended version of DAMMIN) was used to obtain a three phases dummy atom models of the AmtB-DDM complex reporting the protein, DDM head and DDM tail phases respectively. The analysis was done using all SAS (SAXS and SANS at 0, 22, 42 and 60 % D₂O) data. The parameters used for the analysis were 1-the volume of the AmtB trimer (calculated from the amino acid sequence using the *Biomolecular Scattering Length Density Calculator* available on line (<http://pslde.isis.rl.ac.uk/Pslde>)). The volume obtained was 166,864 Å³. 2-the volume of the 320 molecules of DDM head and tail (112,000 Å³ and 108,800 Å³ respectively)³⁰. The SEC-MALS, AUC and SAXS analysis shows that AmtB is trimeric (Table S1), hence a P3 symmetry constraint was applied. The MONSA analysis (200 annealing steps) were done using DAMESV²⁸⁻²⁹ models. 10 model were generated, superimposed and checked for consistency (Figure S9). All models were very similar in size and shape for all three phases.

References

- (1) Zheng, L.; Kostrewa, D.; Bernšche, S.; Winkler, F. K.; Li, X. D., The mechanism of ammonia transport based on the crystal structure of AmtB of *E. coli* *Proc. Natl. Acad. Sci. U.S.A.* **2004**, *101*, 17090-17095.
- (2) Slotboom, D. J.; Duurkens, R. H.; Olieman, K.; Erkens, G. B., Static light scattering to characterize membrane proteins in detergent solution. *Methods* **2008**, *46*, 73-82.
- (3) Schuck, P., Size-distribution analysis of macromolecules by sedimentation velocity ultracentrifugation and lamm equation modeling. *Biophys. J.* **2000**, *78*, 1606-1619.
- (4) Ebel, C., Sedimentation velocity to characterize surfactants and solubilized membrane proteins. *Methods* **2011**, *54*, 56-66.
- (5) Fisher, E.; Zhao, Y.; Richardson, R.; Janik, M.; Buell, A. K.; Aigbirhio, F. I.; Toth, G., Detection and Characterization of Small Molecule Interactions with Fibrillar Protein Aggregates Using Microscale Thermophoresis. *ACS Chem. Neurosci.* **2017**, *8*, 2088-2095.
- (6) Trewthella, J.; Duff, A. P.; Durand, D.; Gabel, F.; Guss, J. M.; Hendrickson, W. A.; Hura, G. L.; Jacques, D. A.; Kirby, N. M.; Kwan, A. H.; Perez, J.; Pollack, L.; Ryan, T. M.; Sali, A.; Schneidman-Duhovny, D.; Schwede, T.; Svergun, D. I.; Sugiyama, M.; Tainer, J. A.; Vachette, P.; Westbrook, J.; Whitten, A. E., 2017 publication guidelines for structural modelling of small-angle scattering data from biomolecules in solution: an update. *Acta Crystallogr. D. Struct. Biol.* **2017**, *73*, 710-728.
- (7) Jeffries, C. M.; Graewert, M. A.; Blanchet, C. E.; Langley, D. B.; Whitten, A. E.; Svergun, D. I., Preparing monodisperse macromolecular samples for successful biological small-angle X-ray and neutron-scattering experiments. *Nat. Protoc.* **2016**, *11*, 2122-2153.
- (8) Khademi, S.; O'Connell, J., III; Remis, J.; Robles-Colmenares, Y.; Miercke, L. J.; Stroud, R. M., Mechanism of ammonia transport by Amt/MEP/Rh: structure of AmtB at 1.35 Å. *Science* **2004**, *305*, 1587-1594.
- (9) Lee, J.; Cheng, X.; Swails, J. M.; Yeom, M. S.; Eastman, P. K.; Lemkul, J. A.; Wei, S.; Buckner, J.; Jeong, J. C.; Qi, Y.; Jo, S.; Pande, V. S.; Case, D. A.; Brooks, C. L., 3rd; MacKerell, A. D., Jr.; Klauda, J. B.; Im, W., CHARMM-GUI Input Generator for NAMD, GROMACS, AMBER, OpenMM, and CHARMM/OpenMM Simulations Using the CHARMM36 Additive Force Field. *J. Chem. Theory. Comput.* **2016**, *12*, 405-413.
- (10) Brooks, B. R.; Brooks, C. L., 3rd; Mackerell, A. D., Jr.; Nilsson, L.; Petrella, R. J.; Roux, B.; Won, Y.; Archontis, G.; Bartels, C.; Boresch, S.; Caflisch, A.; Caves, L.; Cui, Q.; Dinner, A. R.; Feig, M.; Fischer, S.; Gao, J.; Hodoscek, M.; Im, W.; Kuczera, K.; Lazaridis, T.; Ma, J.; Ovchinnikov, V.; Paci, E.; Pastor, R. W.; Post, C. B.; Pu, J. Z.; Schaefer, M.; Tidor, B.; Venable, R. M.; Woodcock, H. L.; Wu, X.; Yang, W.; York, D. M.; Karplus, M., CHARMM: the biomolecular simulation program. *J. Comput. Chem.* **2009**, *30*, 1545-1614.
- (11) Jo, S.; Lim, J. B.; Klauda, J. B.; Im, W., CHARMM-GUI Membrane Builder for mixed bilayers and its application to yeast membranes. *Biophys. J.* **2009**, *97*, 50-58.
- (12) Jo, S.; Kim, T.; Im, W., Automated builder and database of protein/membrane complexes for molecular dynamics simulations. *PLoS One* **2007**, *2*, e880.
- (13) Abraham, M. J., Performance enhancements for GROMACS nonbonded interactions on BlueGene. *J. Comput. Chem.* **2011**, *32*, 2041-2046.
- (14) Berendsen, H. J. C.; van der Spoel, D.; van Drunen, R., GROMACS: A message-passing parallel molecular dynamics implementation. *Comput. Phys. Commun.* **1995**, *91*, 43-56.
- (15) Best, R. B.; Zhu, X.; Shim, J.; Lopes, P. E.; Mittal, J.; Feig, M.; Mackerell, A. D., Jr., Optimization of the additive CHARMM all-atom protein force field targeting improved

sampling of the backbone phi, psi and side-chain chi(1) and chi(2) dihedral angles. *J. Chem. Theory Comput.* **2012**, *8*, 3257-3273.

(16) Klauda, J. B.; Venable, R. M.; Freites, J. A.; O'Connor, J. W.; Tobias, D. J.; Mondragon-Ramirez, C.; Vorobyov, I.; MacKerell, A. D., Jr.; Pastor, R. W., Update of the CHARMM all-atom additive force field for lipids: validation on six lipid types. *J. Phys. Chem. B* **2010**, *114*, 7830-7843.

(17) MacKerell, A. D.; Bashford, D.; Bellott, M.; Dunbrack, R. L.; Evanseck, J. D.; Field, M. J.; Fischer, S.; Gao, J.; Guo, H.; Ha, S.; Joseph-McCarthy, D.; Kuchnir, L.; Kuczera, K.; Lau, F. T.; Mattos, C.; Michnick, S.; Ngo, T.; Nguyen, D. T.; Prodhom, B.; Reiher, W. E.; Roux, B.; Schlenkrich, M.; Smith, J. C.; Stote, R.; Straub, J.; Watanabe, M.; Wiorkiewicz-Kuczera, J.; Yin, D.; Karplus, M., All-atom empirical potential for molecular modeling and dynamics studies of proteins. *J. Phys. Chem. B* **1998**, *102*, 3586-3616.

(18) Miyamoto, S.; Kollman, P. A., Settle: An analytical version of the SHAKE and RATTLE algorithm for rigid water models. *J. Comput. Chem.* **1992**, *13*, 952-962.

(19) Hess, B.; Bekker, H.; Berendsen, H. J. C.; Fraaije, J. G. E. M., LINCS: A linear constraint solver for molecular simulations. *J. Comput. Chem.* **1997**, *18*, 1463-1472.

(20) Berendsen, H. J. C.; Postma, J. P. M.; van Gunsteren, W. F.; DiNola, A.; Haak, J. R., Molecular dynamics with coupling to an external bath. *J. Chem. Phys.* **1984**, *81*, 3684-3690.

(21) Bussi, G.; Donadio, D.; Parrinello, M., Canonical sampling through velocity rescaling. *J. Chem. Phys.* **2007**, *126*, 014101.

(22) Chen, P. C.; Hub, J. S., Validating solution ensembles from molecular dynamics simulation by wide-angle X-ray scattering data. *Biophys. J.* **2014**, *107*, 435-447.

(23) Knight, C. J.; Hub, J. S., WAXSiS: a web server for the calculation of SAXS/WAXS curves based on explicit-solvent molecular dynamics. *Nucleic. Acids. Res.* **2015**, *43*, 225-230.

(24) Jacrot, B., The study of biological structures by neutron scattering in solution. *Rep. Prog. Phys.* **1976**, *39*, 42-56.

(25) Svergun, D. I.; Richard, S.; Koch, M. H.; Sayers, Z.; Kuprin, S.; Zaccai, G., Protein hydration in solution: experimental observation by x-ray and neutron scattering. *Proc. Natl. Acad. Sci. USA* **1998**, *95*, 2267-2272.

(26) Franke, D.; Petoukhov, M. V.; Konarev, P. V.; Panjkovich, A.; Tuukkanen, A.; Mertens, H. D. T.; Kikhney, A. G.; Hajizadeh, N. R.; Franklin, J. M.; Jeffries, C. M.; Svergun, D. I., ATSAS 2.8: a comprehensive data analysis suite for small-angle scattering from macromolecular solutions. *J. Appl. Crystallogr.* **2017**, *50*, 1212-1225.

(27) Compton, E. L.; Karinou, E.; Naismith, J. H.; Gabel, F.; Javelle, A., Low resolution structure of a bacterial SLC26 transporter reveals dimeric stoichiometry and mobile intracellular domains. *J. Biol. Chem* **2011**, *286*, 27058-27067.

(28) Reyes, F. E.; Schwartz, C. R.; Tainer, J. A.; Rambo, R. P., Methods for using new conceptual tools and parameters to assess RNA structure by small-angle X-ray scattering. *Methods Enzymol.* **2014**, *549*, 235-263.

(29) Svergun, D. I., Restoring low resolution structure of biological macromolecules from solution scattering using simulated annealing. *Biophys. J.* **1999**, *76*, 2879-2886.

(30) Breyton, C.; Gabel, F.; Lethier, M.; Flayhan, A.; Durand, G.; Jault, J. M.; Juillan-Binard, C.; Imbert, L.; Moulin, M.; Ravaud, S.; Hartlein, M.; Ebel, C., Small angle neutron scattering for the study of solubilised membrane proteins. *Eur. Phys. J. E. Soft Matter* **2013**, *36*, 71-86.

Supporting Tables and Figures

Table S1: Determination of the number of DDM molecules in the AmtB-DDM complex.*

| | M_w AmtB-DDM | M_w AmtB/oligomeric state | M_w DDM | DDM molecules |
|--------------------------------------|----------------|-----------------------------|-----------|---------------|
| SEC-MALS | 287.2±16.7 | 144.4±11.1 / trimer | 142.8±5.9 | 285±12 |
| AUC | 312.6±14.5 | 148.8±6.8 / trimer | 163.7±0.7 | 321±1 |
| SANS (I_0) (22%D ₂ O) | n.a. | 146.0±29.2 / trimer | n.a. | n.a. |

*Molecular mass in kDa.

Table S2: SEC-SAXS and SANS data-collection parameters.

| | from SEC-SAXS | | from SANS batch | |
|--|---------------|--|----------------------------|--|
| Instrument/data processing | B21 | BioSAXS Diamond Light Source synchrotron beamline (UK) | D22 beamline | Institut Laue-Langevin Neutron source with a multidetector (3He) 16K resolution elements |
| Beam geometry (mm) | 1 | X 5 | 55 | x 40 |
| Camera length (m) | 4.014 | | 4/4 | offset |
| Flow (ml/min) | 0.05 | | N/A | |
| Wavelength (Å) | 0.99 | | 6.0 | ($\Delta\lambda/\lambda = 10\%$) |
| s range (Å⁻¹) | 0.0022 | to 0.42 | 0.045 | to 0.4 |
| Exposure time (s) | 3 | (every 5 seconds) | ~3600 | to 10800/sample |
| Sample configuration | | | cell path-length of 1 mm | |
| Concentration (mg·mL⁻¹) | range | see supporting information | see supporting information | |
| Temperature (K) | 298 | | 279.15 | |

Table S3: R_g^* calculated from Guinier approximation of the experimental and computed SAXS curves of the AmtB-DDM complex containing between 260 and 360 DDM molecules.

| 260 | 280 | 300 | 320 | 340 | 360 | Experimental SAXS data |
|-----------|-----------|-----------|------------------|-----------|-----------|------------------------|
| 43.1±0.24 | 44.0±0.30 | 44.5±0.26 | 45.6±0.10 | 47.8±0.16 | 48.6±0.13 | 45.5±0.09 |

* R_g express in Å

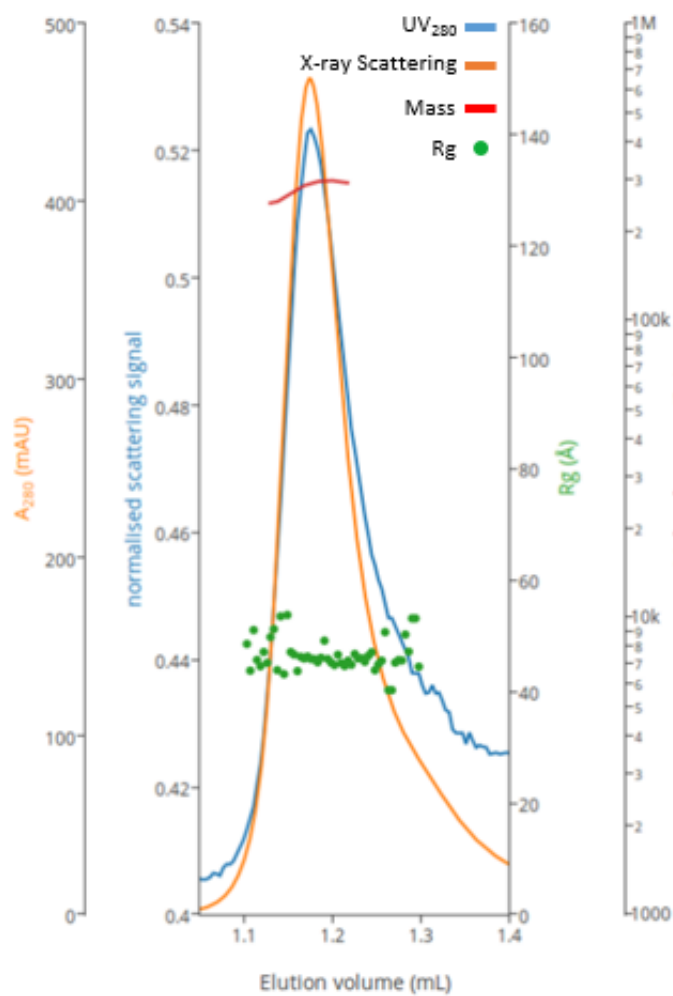


Figure S1: Elution profile of AmtB purified in 0.03% DDM from a superdex 200 10x300 column measured by OD at 280nm and scattering.

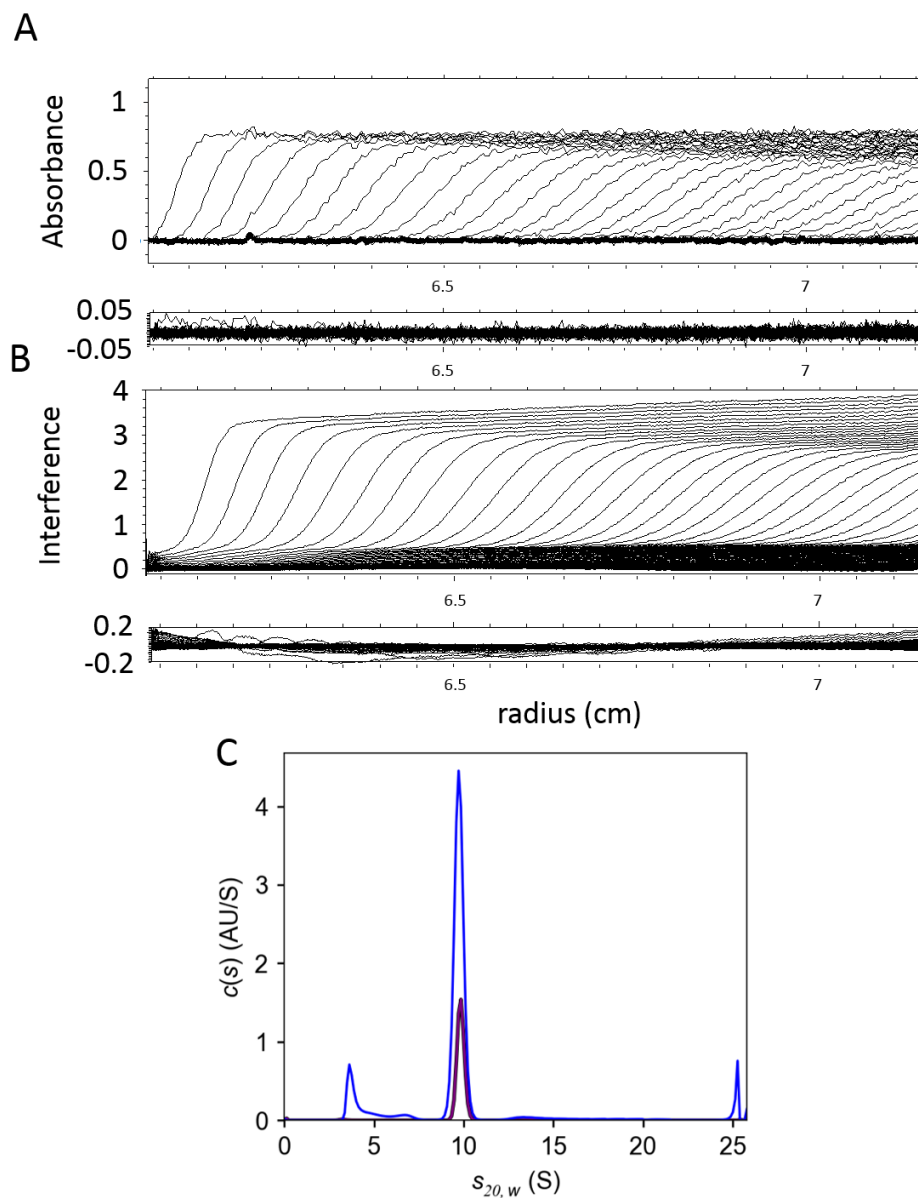


Figure S2: (A) Absorbance at 280nm and (B) interference signals of analytical ultracentrifugation sedimentation profile of AmtB solubilised in 0.03% DDM. (C) Superposition of the $c(s)$ distributions expressed at 20°C in water (blue: A_{280nm} , purple: Interference).

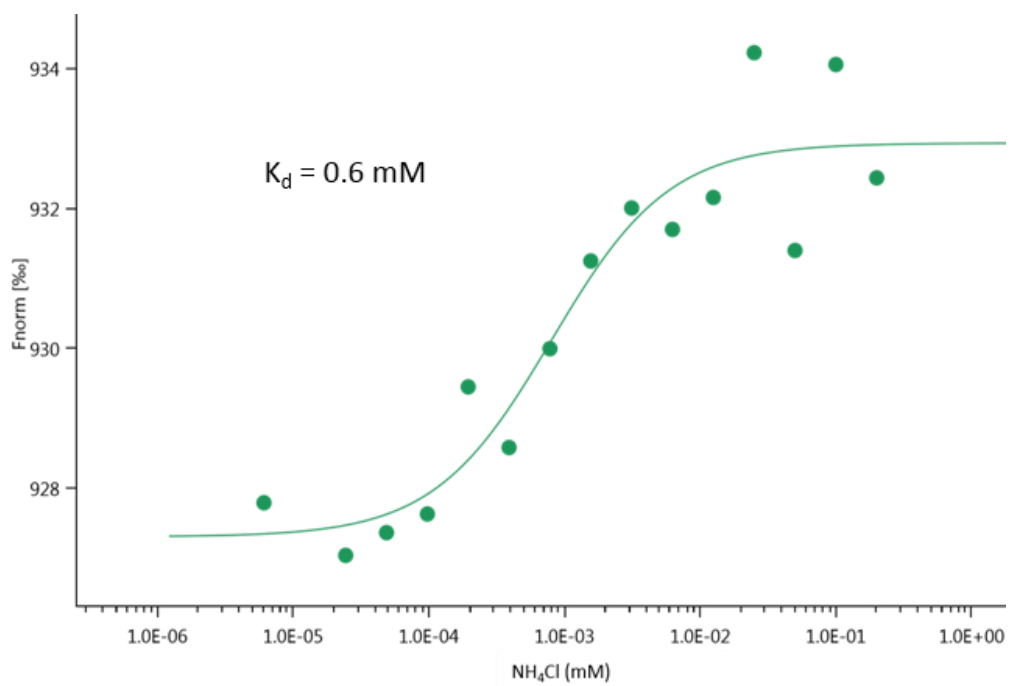


Figure S3: Measurement of the ammonium binding on AmtB solubilised in 0.03% DDM by microscale thermophoresis.

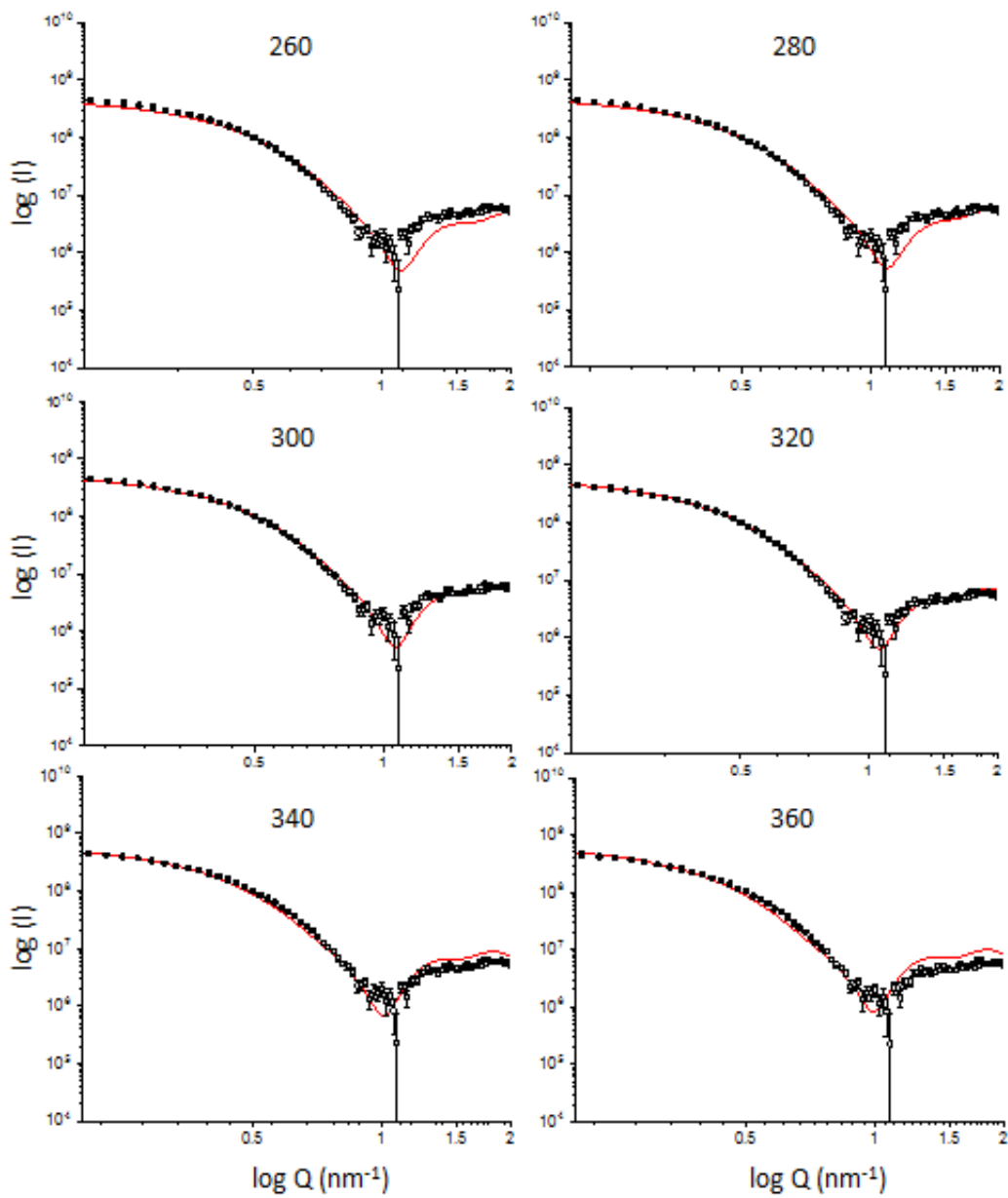


Figure S4: Comparison of the SAXS curves from experiment (symbols) and computed from MD simulations of the AmtB-DDM complex containing between 260 and 360 DDM molecules (red lines).

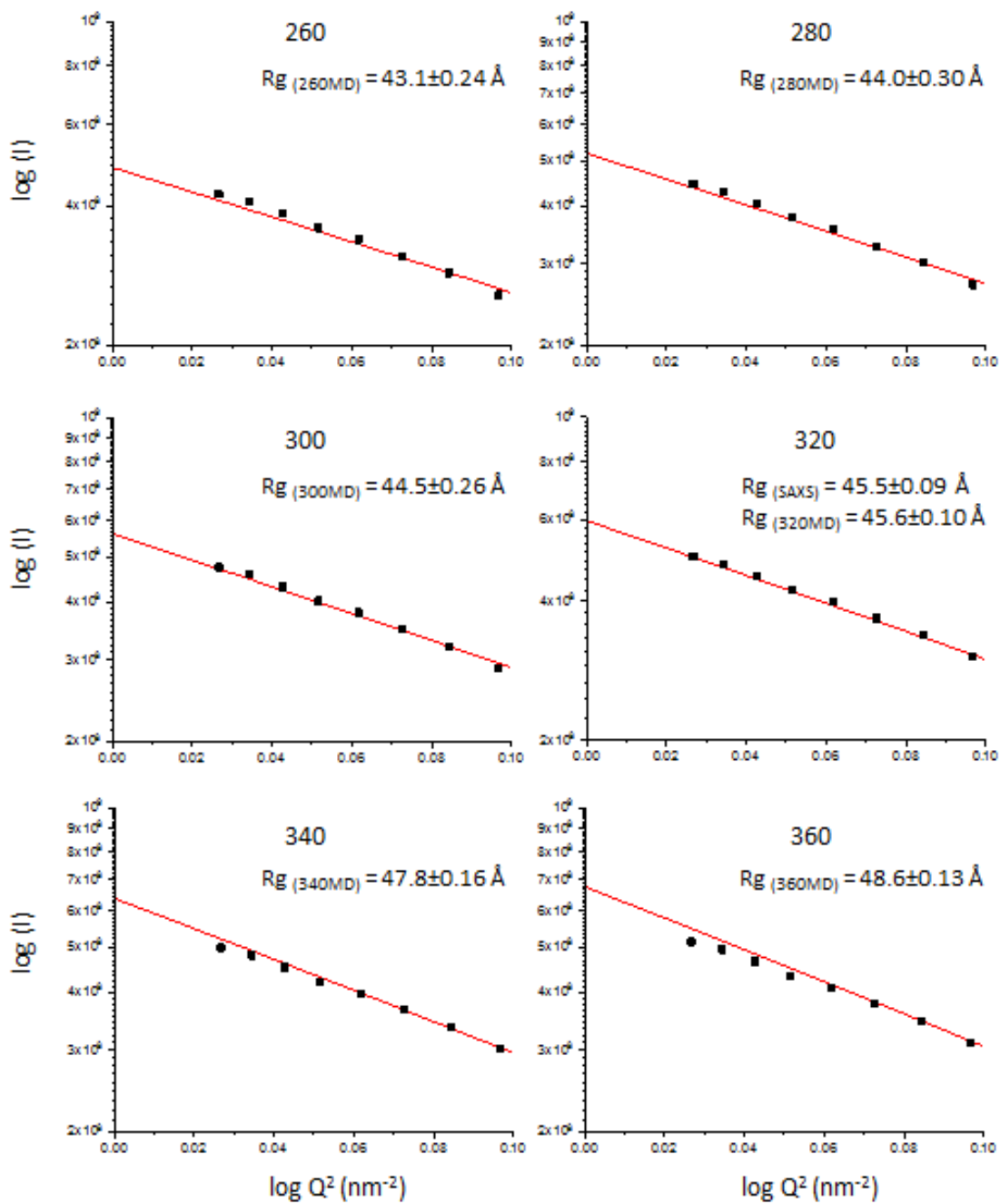


Figure S5: Guinier plot comparison of the experimental (symbols) and computed (red line) SAXS curves of the AmtB-DDM complex containing between 260 and 360 DDM molecules.

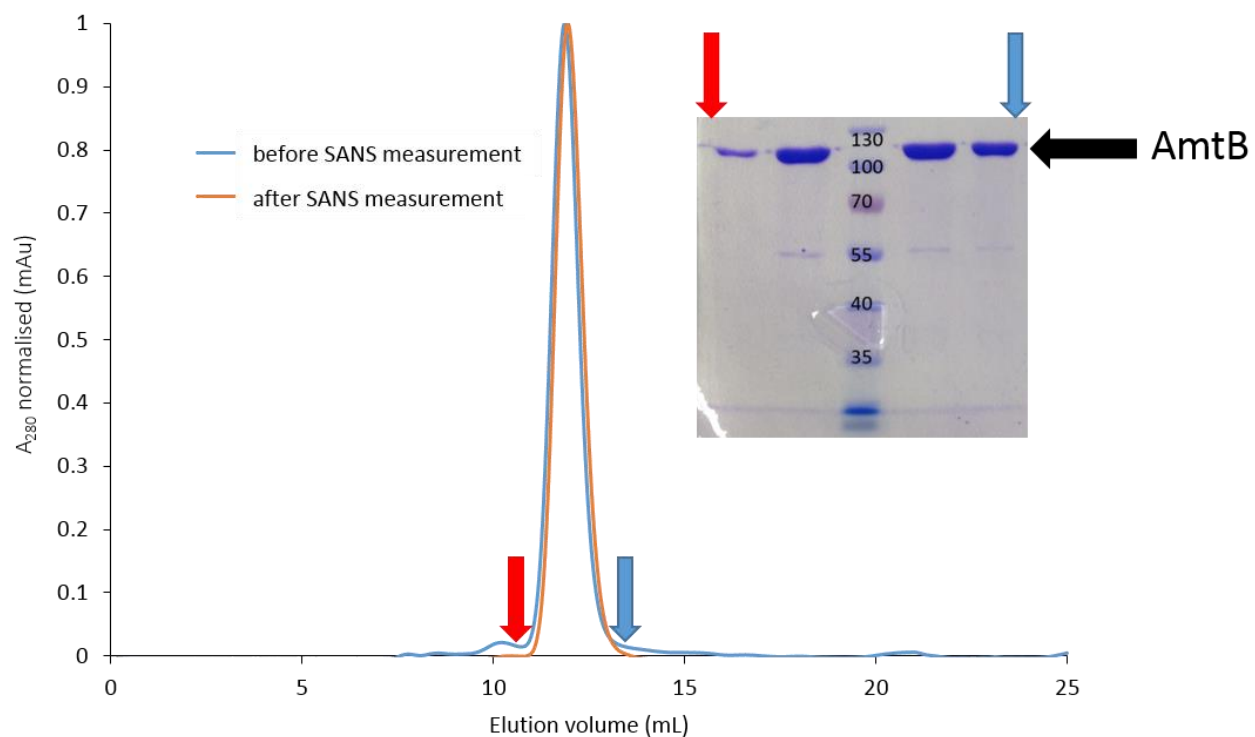


Figure S6: Size exclusion chromatography profile of AmtB solubilised in 0.03% DDM, 0% D₂O, before and after SANS experiments. Before SANS measurement, peak elution 11.87 ml and after SANS measurement, peak elution 11.96 ml. (*insert*) 12.5% SDS-PAGE fraction analysis based of the elution peak.

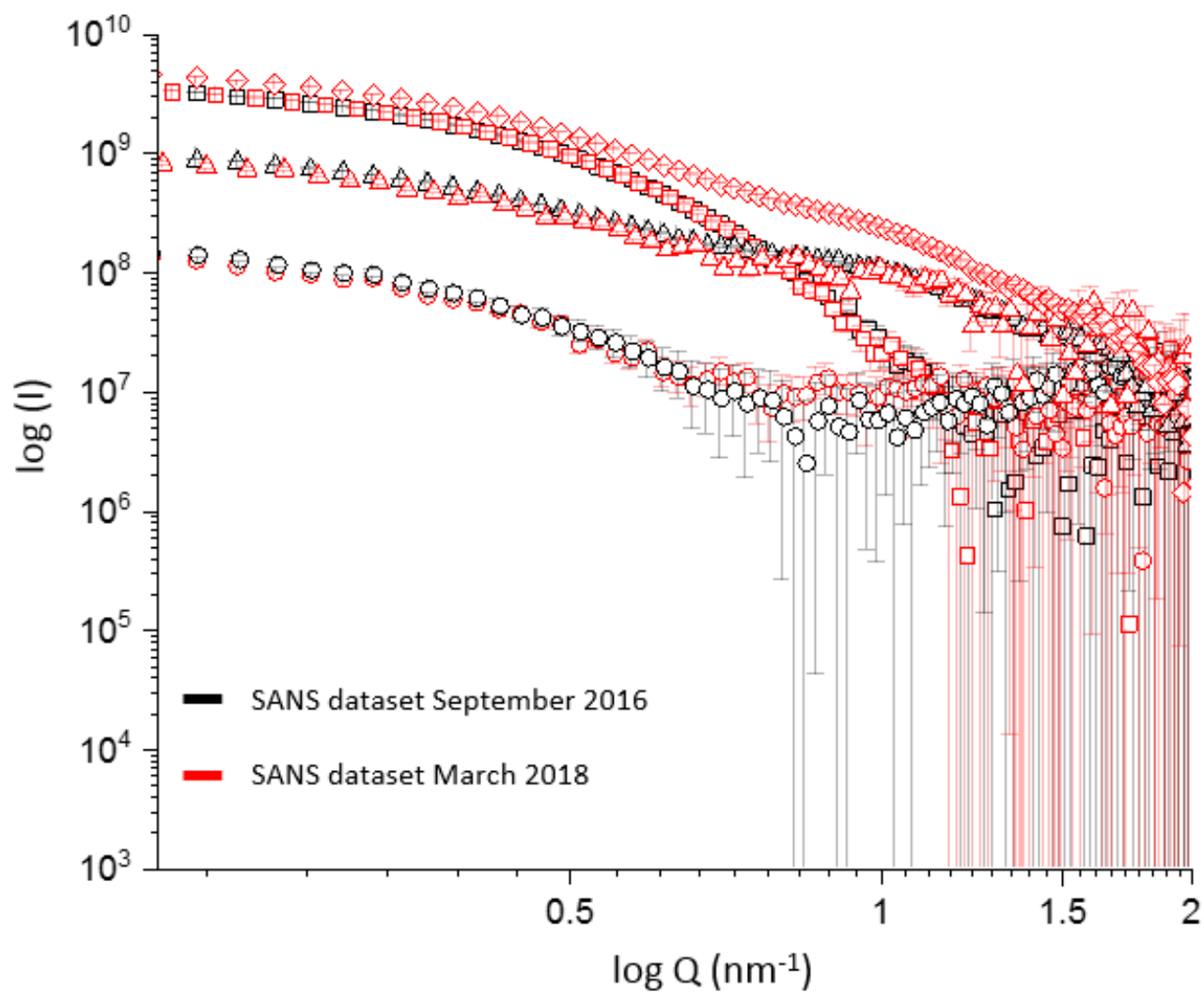


Figure S7: Comparison of the two SANS dataset. (\square) 0% D_2O , (\circ) 22% D_2O , (\triangle) 42% D_2O . The dataset at (\diamond) 60% D_2O have only been measured in March 2018.

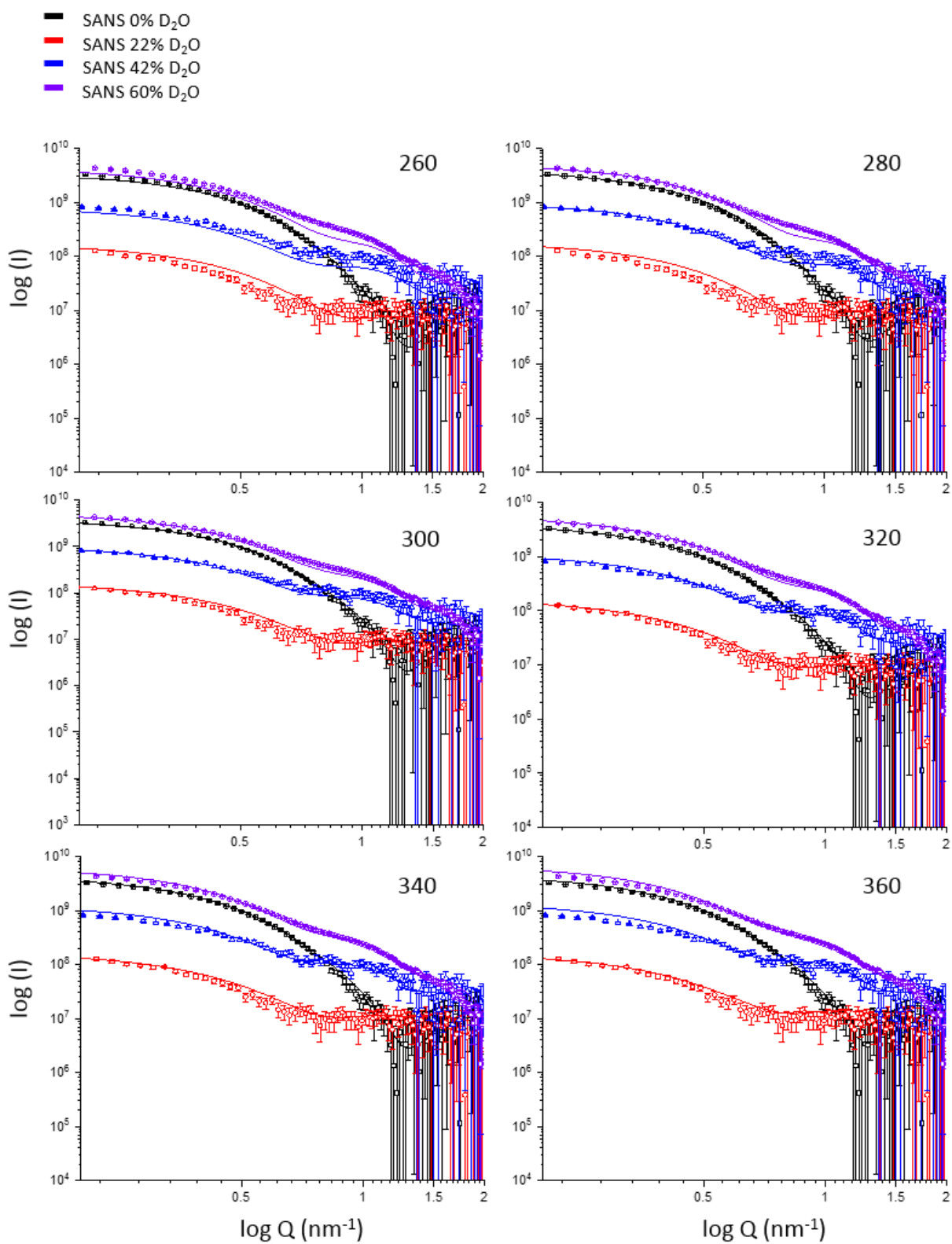


Figure S8: Comparison of experimental (symbols) and computed (lines) SANS curves from MD simulations containing between 260 and 360 DDM molecules.

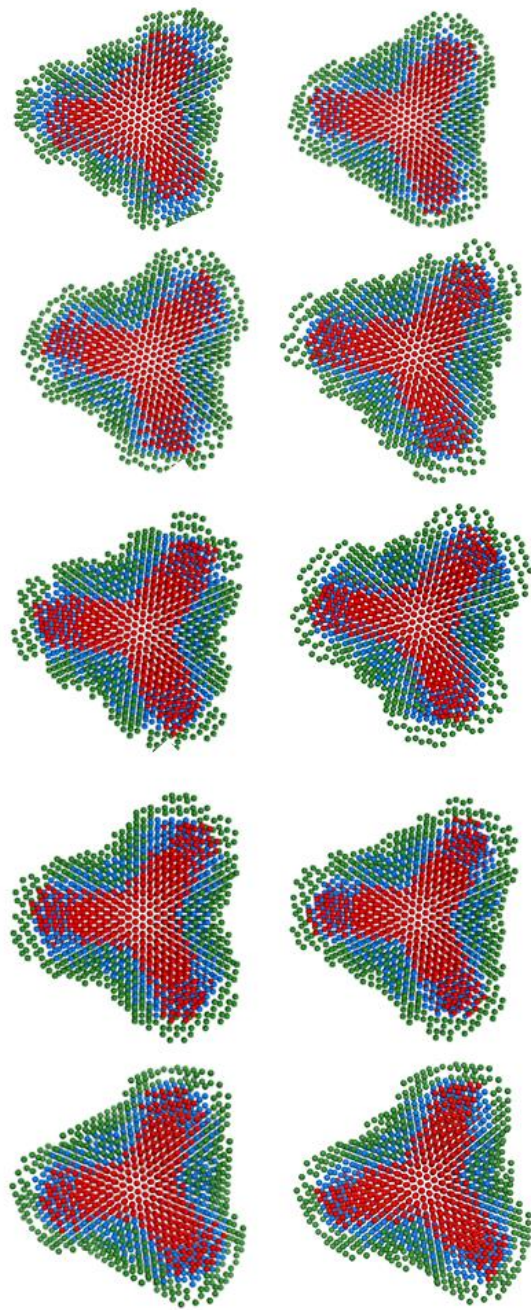


Figure S9: Top view of 10 different MONSA multiphase modelling using the SAXS and SANS data. The phase corresponding to the protein is represented by red beads, the hydrophilic and hydrophobic detergent density are represented by green and blue beads, respectively.